# A CLOSED FORM SOLUTION FOR THE FREE VIBRATIONAL CHARACTERISTICS OF A ROTATING DISK – SPINDLE SYSTEM

**Abdul Kareem Abdul Rezzak** **Ahmed Abdullah Al Rajihy**
*Mechanical Engineering Department, University of Babylon*

## Abstract

Rotating disk – spindle system consists of an elastic disk mounted on an elastic spindle by means of rigid clamp. This work presents a closed form solution for the eigensolutions of such systems. The complex eigenfunctions have the classical properties of a gyroscopic system when the individual disc, spindle and clamp deflections for a given eigenfunction are collected in terms of an extended eigenfunction. Critical speeds analogous to those of rigidly supported (classical) rotating disk are examined for the coupled system. It is concluded that whereas the rigidly supported disc does not experience critical speed instability in the one – nodal diameter eigenfunctions, the coupled system does.

## Introduction

An extensive literatures on the vibration and stability of spindle (short rotating shaft) and rotating disks have been published in the last several decades. Analyses that model elastic continuous system vibration typically focus on either the spindle (with any attached disks modeled as rigid) or the disk (supported by a rigid structure).

Practical systems such as disk drives, turbo machinery and high speed gear systems, however, exhibit coupled disc – spindle response wherein dynamic excitation at either the disk or spindle excites elastic vibration of both components. For example, the predominant excitation in gears is at the tooth mesh, but an acceptable noise is radiated primarily from the housing. The vibratory response is a coupled one involving the disk, spindle, bearings and housing. The reverse path occurs in disk drives where bearing forces and support structure motion drive disk vibration. While focusing on decoupled models, the existing literature also emphasizes free vibration and stability investigations with considerably less attention to the operating condition response.

J.A. Dopkin and T.E. Shoup [2], D.R. Chivens and H.D. Nelson [3] and F.S. Wu and G.T. Flowers [4] generally use transfer matrix method and other lumped models to examine natural frequencies and critical speeds. Their methods are focused on turbo machinery applications. None of these studies examine modal coupling and forced response. Chivens and Nelson [3] analytically studied the natural frequencies of an elastic disk – spindle system coupled by thin clamp. They conclude that disk flexibility alters the natural frequencies of an elastic spindle – rigid disk system but not the critical speeds.

The present work builds on that of Chivens and Nelson [3[and Parker [1].

## Theoretical Approach

This study examines a coupled disk – spindle system where both the disk and the spindle are elastic bodies, a rigid clamp, Fig. (1), couples them. The associated eigenvalue problem is analytically solved in closed form solution (CFS) for the natural frequencies, vibration mode and critical speeds.

## (A) Equations Of Motion

Figure (1) shows the disk – spindle system, in which an elastic, axisymmetric, rotating cantilever spindle carries elastic, axisymmetric disk at its end and rigid clamp couples these components. The deformation is described by seven variables namely, w(r,θ,t), u(z,t), v(z,t), $u^c(t)$, $v^c(t)$, φ(t) and ψ(t). These seven variables are not independent because the clamp motions are related to the spindle deflections by the geometric compatibility conditions:

$$\varphi = \frac{\partial u}{\partial z}\Big| z = l \,,\; \psi = \frac{\partial v}{\partial z}\Big| z = l \,,\; u^c = u\big| z = l + d_1\varphi \,,\; v^c = v\big| z = l + d_1\psi \quad \ldots(1)$$

The dimensionless parameters of the system are:

$$t = t^{-}\sqrt{\frac{EI}{\rho_s l^4}} \,,\; \Omega = \Omega^{-}\sqrt{\frac{\rho_s l^4}{EI}} \,,\; d_1 = \frac{d_1^{-}}{l} \,,\; K = \frac{D}{EI} l \,,\; \rho = \frac{\rho_d b^2}{\rho_s l^3} \,,\; \alpha = \frac{m}{\rho_s l} \,,\; \gamma = \frac{a}{b} \,,$$

$$J_{ii}^{c,d} = \frac{J_{ii}^{-c,d}}{\rho_s l^3} \,,\; q_d = \frac{q_d^{-}}{EI} l b^3 \,,\; q_{u,v} = \frac{q_{u,v}^{-}}{EI} l^3 \,,\; F_i = \frac{F_i^{-}}{EI} l^2 \,,\; M_i = \frac{M_i^{-}}{EI} l \quad \ldots(2)$$

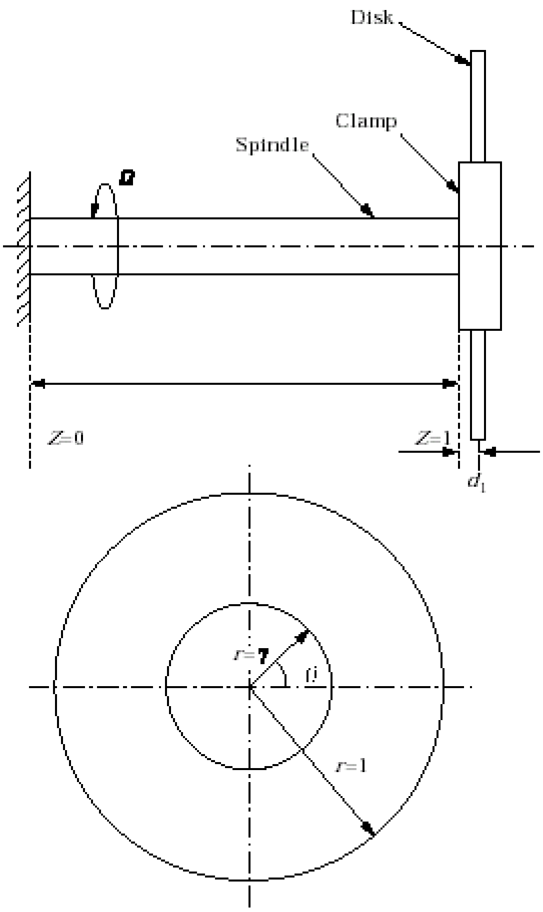


**Figure(1): Rotating disk – spindle system**

Parker [1] derived the linearized equations of motion of the system in rotating co-ordinates as follows:
The governing equation over the continuous disk domain is:

$$K\nabla^4 w - \Omega^2 \xi(w) + \rho(\frac{\partial^2 w}{\partial t^2} - r\cos\theta(\frac{\partial \varphi}{\partial t} + \Omega^2 \varphi) - r\sin\theta(\frac{\partial \psi}{\partial t} + \Omega^2 \psi)) = q_d(r,\theta,t) \ldots(3)$$

, the governing equations over the continuous spindle domain are:

$$\frac{\partial^4 u}{\partial z^4} + \frac{\partial^2 u}{\partial t^2} - 2\Omega \frac{\partial v}{\partial t} - \Omega^2 u = q_u(z,t) \quad \ldots(4)$$

$$\frac{\partial^4 v}{\partial z^4} + \frac{\partial^2 v}{\partial t^2} + 2\Omega \frac{\partial u}{\partial t} - \Omega^2 v = q_v(z,t) \quad \ldots(5)$$

, the linear momentum balance equations for the clamp are:

$$\alpha \frac{\partial^2 u^c}{\partial t^2} - \frac{\partial^3 u}{\partial z^3}|z = l - 2\Omega\alpha \frac{\partial v^c}{\partial t} - \Omega^2 \alpha u^c = F_1(t) \quad \ldots(6)$$

$$\alpha \frac{\partial^2 v^c}{\partial t^2} - \frac{\partial^3 v}{\partial z^3}|z = l + 2\Omega\alpha \frac{\partial u^c}{\partial t} - \Omega^2 \alpha v^c = F_2(t) \quad \ldots(7)$$

and the angular momentum balance equations for the clamp are:

$$\frac{\partial^2 u}{\partial z^2}|z = l + d_1 \frac{\partial^3 u}{\partial z^3}|z = l + (J_{22}^c + J_{22}^d)\frac{\partial^2 \varphi}{\partial t^2} - \iint \rho r\cos\theta \frac{\partial^2 w}{\partial t^2} dA - \Omega(J_{11}^c + J_{22}^c - J_{33}^c)\frac{\partial \psi}{\partial t} -$$
$$\Omega^2((J_{11}^c - J_{33}^c - J_{22}^d)\varphi + \iint \rho r\cos\theta w dA) = M_2(t) \quad \ldots(8)$$

$$\frac{\partial^2 v}{\partial z^2}|z = l + d_1 \frac{\partial^3 v}{\partial z^3}|z = l + (J_{11}^c + J_{11}^d)\frac{\partial^2 \psi}{\partial t^2} - \iint \rho r\sin\theta \frac{\partial^2 w}{\partial t^2} dA + \Omega(J_{11}^c + J_{22}^c - J_{33}^c)\frac{\partial \varphi}{\partial t} -$$
$$\Omega^2((J_{22}^c - J_{33}^c - J_{11}^d)\psi + \iint \rho r\sin\theta w dA) = -M_1(t) \quad \ldots(9)$$

Here r and θ are polar co- ordinates in the frame fixed to the rotating disk , z is the co- ordinate of a material point on the spindle and ξ(w) is the membrane stress operator [5]

$$\Omega^2 \xi(w) = \frac{1}{r}\frac{\partial}{\partial r}(r\sigma^r w_r) + \frac{1}{r}\frac{\partial}{\partial \theta}(\sigma^\theta w_\theta) \quad \ldots(10)$$

Where

$$\sigma^r = \Omega^2(c_1 + \frac{c_2}{r^2} + c_3 r^2),\ \sigma^\theta = \Omega^2(c_1 - \frac{c_2}{r^2} + c_4 r^2) \ldots(11)$$

Where

$$c_1 = \rho(\frac{1+\upsilon}{8})\frac{(\upsilon-1)\gamma^4 - (3+\upsilon)}{(\upsilon-1)\gamma^2 - (1+\upsilon)},\ c_2 = \rho(\frac{1-\upsilon}{8})\upsilon^2 \frac{(\upsilon+1)\gamma^2 - (3+\upsilon)}{(\upsilon-1)\gamma^2 - (1+\upsilon)}$$

$$c_3 = -\rho(\frac{3+\upsilon}{8}) \text{ and } c_4 = -\rho(\frac{1+3\upsilon}{8}) \quad \ldots(12)$$

The spindle and disk boundary conditions are:

$$u|z = 0 = v|z = 0 = 0,\ \frac{\partial u}{\partial z}\Big|z = 0 = \frac{\partial v}{\partial z}|z = 0,\ w|r = \gamma = 0,\ \frac{\partial w}{\partial r}|r = \gamma = 0$$

$$(\nabla^2 w - \frac{1-\upsilon}{r}(\frac{\partial w}{\partial r} + \frac{1}{r}\frac{\partial^2 w}{\partial \theta^2}))|r = 1 = 0,\ (\frac{\partial}{\partial r}\nabla^2 w - \frac{1-\upsilon}{r^2}(\frac{1}{r}\frac{\partial^2 w}{\partial \theta^2} - \frac{\partial}{\partial r}\frac{\partial^2 w}{\partial \theta^2}))|r = 1 = 0 \quad \ldots(13)$$

Equations (3) – (9) can be written in the structured manner using the extended operator formulation [1].

Defining the extended variable $\bar{h}$ as

$$\bar{h}(r,\theta,z,t) = \left[w(r,\theta,t)u(z,t)v(z,t)u^c(t)v^c(t)\varphi(t)\psi(t)\right]^T \quad \ldots(14)$$

Equations (3) – (9) are written concisely as

$$\bar{M}\frac{\partial \bar{h}}{\partial t}+\Omega\bar{G}\frac{\partial \bar{h}}{\partial t}+(\bar{L}-\Omega^2\bar{\bar{L}})\bar{h}=\bar{f} \quad \ldots(15)$$

where $\bar{M}$, $\bar{G}$, $\bar{L}$ and $\bar{\bar{L}}$ are the extended operators operating on $\bar{h}$ and $\bar{f}$ is the extended excitation vector. These operators are defined in [1].

The inner product between two extended variables x and y is defined as

$$(x\ ,\ y)=\iint x_1\bar{y}_1 dA+\int_0^1 x_2\bar{y}_2 dz+\int_0^1 x_3\bar{y}_3 dz+x_4\bar{y}_4+x_5\bar{y}_5+x_6\bar{y}_6+x_7\bar{y}_7 \quad \ldots(16)$$

where $x_i$ and $y_i$ are the elements of the extended variables x and y, the double integral is over the area of the disk and, single integrals are over the length of the spindle and the over bar denotes complex conjugate. With this inner product and with the constraint (equations. 1), the operators $\bar{M}$, $\bar{L}$ and $\bar{\bar{L}}$ are symmetric and $\bar{G}$ is skew – symmetric. Moreover $\bar{M}$ and $\bar{L}$ are positive definite. Thus equations (15) and (16) cast the disk – spindle system in the canonical form of gyroscopic continuum. The importance of this structured formulation will be evident in the perturbation analysis and the forced response discussed later.

## (B) Closed Form Solution of the Eigenvalue Problem

A closed form solution (CFS) of the gyroscopic system eigenvalue problem is presented here. Using the separation of variables technique

$u(z,t)=\zeta(z)e^{\lambda t}$ and $v(z,t)=\eta(z)e^{\lambda t}$

in the spindle equations (4) and (5) gives

$$\frac{\partial^4\zeta}{\partial z^4}+\lambda^2\zeta-2\Omega\lambda\eta-\Omega^2\zeta=0 \quad \ldots(17)$$

$$\frac{\partial^4\eta}{\partial z^4}+\lambda^2\eta+2\Omega\lambda\zeta-\Omega^2\eta=0 \quad \ldots(18)$$

Decoupling these equations yields

$$\frac{d^8\zeta}{dz^8}+2(\lambda^2-\Omega^2)\frac{d^4\zeta}{dz^4}+(\lambda^2+\Omega^2)^2\zeta=0 \quad \ldots(19)$$

and an identical equation for η. The general solution for Eq.(19) is

$$\zeta(z)=A_1\cos\kappa z+A_2\sin\kappa z+A_3\cosh\kappa z+A_4\sinh\kappa z+A_5\cos\beta z+A_6\sin\beta z$$
$$+A_7\cosh\beta z+A_8\sinh\beta z \quad \ldots(20)$$

where $A_i$ are complex constants, $\kappa=(-\lambda^2+\Omega^2+2i\lambda\Omega)^{0.25}$ and $\beta=(-\lambda^2+\Omega^2-2i\lambda\Omega)^{0.25}$. The solution of η(z) is identical to Eq.(20) with $C_i$ instead of $A_i$. Substituting η(z) solution and Eq.(20) into Eq.(17)(or Eq.(18)) yields

$$\eta(z)=-iA_1\cos\kappa z-iA_2\sin\kappa z-iA_3\cosh\kappa z-iA_4\sinh\kappa z+iA_5\cos\beta z+$$
$$iA_6\sin\beta z+iA_7\cosh\beta z+iA_8\sinh\beta z \quad \ldots(21)$$

The eigenfunctions are complex as seen in equations (20) and (21).

Proceeding the separation of variables technique on w(r,θ,t) such that

$w(r,\theta,t)=w(r,\theta)e^{\lambda t}$ reduces equation (3) to

$$K\nabla^4 w-\Omega^2\xi+\rho(\lambda^2(w-r\cos\theta\varphi-r\sin\theta\psi)-\Omega^2(r\cos\theta\varphi r\sin\theta\psi))=0 \quad \ldots(22)$$

For an axisymmetric disk, disk spindle coupling occurs only for the one nodal diameter eigenfunctions [2,6]. These are coupled modes of the system and the only ones of interest here. For numbers of nodal diameters other than one, the deformation is only in the disk; the spindle does not deform. These are the uncoupled modes of the system; they are well known for analyses of rigidly supported disks. For the coupled modes the solution

$w(r,\theta) = g(r)\cos\theta + p(r)\sin\theta$ … (23)

gives the radial part of the disk equation from Eq.(22)

$$r^4\frac{d^4g}{dr^4} + 2r^3\frac{d^3g}{dr^3} - (3r^2 + \delta^2(c_1r^4 + c_2r^2 + c_3r^6))\frac{d^2g}{dr^2} + (3r - \delta^2(c_1r^3 - c_2r + c_4r^5 - \rho r^5))$$
$$\frac{dg}{dr} - (3 - \delta^2(c_1r^2 - c_2 + c_4r^4) + r^4\omega^2(\frac{\rho}{k}))g = \delta^2\rho r^5\varphi - \omega^2(\frac{\rho}{k})r^5\varphi \quad \ldots(24)$$

Where $\delta = \frac{\omega}{\sqrt{K}}$ and $\lambda = i\omega$. An identical solution is obtained from p(r) with $\psi$ instead of $\varphi$. The solution of Eq.(24) is obtained using the power series method [13]. Using an expansion about the ordinary point r=1, the homogeneous solution has the form

$$g(r) = \sum_{i=0}^{\infty} a_i(1-r)^i \quad \ldots \quad (25)$$

Substituting the above equation in the homogeneous form of Eq.(24) and equating coefficients of each power of (1-r) to zero, it is found that the coefficients ($a_0$-$a_3$) are arbitrary, ($a_4$-$a_7$) depends on ($a_0$-$a_3$) and each of the higher coefficients depends on the previous eight coefficients.

The recursion relation for $i \geq 4$ is

$$\begin{aligned}
a_{i+4} = &-[-\{4(i+3)(i+2)(i+1)i + 2(i+3)(i+2)(i+1)\}a_{i+3} + \{6(i+2)(i+1)i(i-1) + \\
&6(i+2)(i+1)i + (-3-\delta^2(c_1+c_2+c_3))(i+2)(i+1)\}a_{i+2} + \{-4(i+1)i(i-1)(i-2) - \\
&6(i+1)i(i-1) + (6-\delta^2(-4c_1-2c_2-6c_3))(i+1)i - (3-\delta^2(c_1-c_2+c_4-\rho))(i+1)\}a_{i+1} + \\
&\{i(i-1)(i-2)(i-3) + 2i(i-1)(i-2) + (-3-\delta^2(6c_1+c_2+15c_3))i(i-1) + \\
&(3+\delta^2(-3c_1+c_2-5c_4+5\rho))i + (-3+\delta^2(c_1-c_2+c_4) - \omega^2\rho/K\}a_i + \\
&\{-\delta^2(-4c_1-20c_3)(i-1)(i-2) + \delta^2(3c_1+10c_4-10\rho)(i-1) + \delta^2(-2c_1-4c_4) + \\
&4\omega^2\rho/K\}a_{i-1} + \{-\delta^2(c_1+15c_3)(i-2)(i-3) + \delta^2(-c_1-10c_4+10\rho)(i-2) + \\
&\delta^2(c_1+6c_4) - 6\omega^2\rho/K\}a_{i-2} + \{6\delta^2c_3(i-3)(i-4) + \delta^2(5c_4-5\rho)(i-3) + \\
&(-4\delta^2c_4 + 4\omega^2\rho/K)\}a_{i-3} + \{-\delta^2c_3(i-4)(i-5) + \delta^2(-c_4+\rho)(i-4) + \\
&\delta^2c_4 - \omega^2\rho/K\}a_{i-4}]/[(i+4)(i+3)(i+2)(i+1)] \quad \ldots (26)
\end{aligned}$$

Substitution of $i = 0$ in the recursion relation and setting the coefficients with negative subscript to zero gives the expression of $a_4$ in terms of ($a_0$-$a_3$). Similarly substituting $i = 1$ and the expression of $a_4$ into the recursion relation gives as in terms of ($a_0$-$a_3$). This procedure is repeated to obtain $a_4$-$a_7$ in terms of ($a_0$-$a_3$). Finally, setting one of the coefficients ($a_0$-$a_3$) equal to one and the other three equal to zero at a time in the power series (eq.25) gives four independent – homogeneous solutions $w_{oh1} - w_{oh4}$ of Eq.(24). The general solution of Eq.(23) to the disk equation is

$$\begin{aligned}
w(r,\theta) = &(B_1w_{oh1} + B_2w_{oh2} + B_3w_{oh3} + B_4w_{oh4} + r\varphi)\cos\theta \\
&+ (B_5w_{oh1} + B_6w_{oh2} + B_7w_{oh3} + B_8w_{oh4} + r\psi)\sin\theta \quad \ldots \quad (27)
\end{aligned}$$

where $r\varphi$ is a particular solution of Eq.(24), $B_i$ are complex constants and the p(r) sinθ term of Eq.(23) has been included.

Insertion of equations (20), (21), and (27) into equations (6) – (9), (13) and (1) yields 16 linear, homogeneous equations in the 16 coefficients $A_i$ and $B_i$. Roots of the characteristic determinant give the natural frequencies ω.

The disk modal deflections (equations (27) and (20)) and that of the spindle (Eq.21) are collected into an extended eigenfunctions of form (14) where the modal deflections and rotations of the clamp are calculated from equation (1).

$$\overline{h_m} = \begin{bmatrix} w_m = g_m(r)\cos\theta + p_m(r)\sin\theta \\ \zeta(m) \\ \eta(m) \\ u_m^c = \zeta_m(1) + d_1\zeta_m(1) \\ v_m^c = \eta_m(1) + d_1\eta_m(1) \\ \varphi = \dfrac{d\zeta_m(1)}{dz} \\ \psi = \dfrac{d\eta_m(1)}{dz} \end{bmatrix} \qquad m = 1,2,3,..... \qquad \ldots\ (28)$$

Note that Eq.(28) is the form of complex coupled modes. They occur in complex conjugate pairs. The uncoupled modes, which are real and degenerate, have the form

$$\overline{h_n} = \left[R_n(r)(a_1\cos n\theta + a_2\sin n\theta)000000\right]^T, n \neq 1 \ \ldots\ (29)$$

where $a_1$ and $a_2$ are arbitrary constants. The coupled vibration modes are qualitatively classified as disk modes, in which the strain energy in the disk dominates the total strain energy, and the spindle modes, in which the strain energy in the spindle dominates the total modal strain energy.

The above solution can be specialized to solve two special cases: the zero speed eigenvalue problem (Ω =0) and the critical speed eigenvalue problem to determine the speeds at which an eigenvalue vanishes (ω=0). To distinguish from disk critical speeds introduced later, the term spindle critical speeds is used for speeds with vanishing eigenvalue as these critical speeds exist for a spindle not coupled to a disk. At such spindle critical speeds, static loads in the rotating frame (e.g. a center of mass offset from the rotation axis) excite a resonant condition. The recursion relations for these problems are obtained by substituting Ω=0 or ω=0 into Eq. (26). Homogeneous solutions of the disk equation for the zero speed eigenvalue problems are Bessel functions. For both Ω=0 and ω=0, the following simplifications occur: equations (4) and (5) reduced to decoupled stationary beam equation with well known solution, the spindle deforms in only one plane for each mode, and the order of the characteristic determinant is 8 as opposed to 16 because of this decoupling. All roots ( that is, zero speed natural frequencies and spindle critical speeds) of the characteristic determinant are degenerate and the two associated modes are identical except for the plane of motion.

## (C) Disk Critical Speeds

The spindle critical speeds at which an eigenvalue vanishes area only part of the complete critical speed picture. In addition to these critical speeds derived from the gyroscopic terms in the spindle equation of motion. They are so called disk critical speeds where the name reflects the association with the critical speeds of a classical spinning disk. To understand this concept, first consider the critical speeds of a classical, rigidly supported disk.

The critical speeds of rigidly supported disk are the speeds at which a disk natural frequency in a ground based (inertial) reference plane is zero [10]. At such speeds any constant, stationary force applied to the disk leads to large amplitude resonant response. In a rotating reference frame, the critical speeds are given by $\Omega_{cr} = \frac{\omega_n}{n}$ where $\omega_n$ is the natural frequency in the rotating reference frame and $n \neq 0$ is the number of nodal diameters in the associated mode. To see the relationship between the fixed and rotating frame characterizations, consider a stationary point force of unit magnitude acting on the disk perpendicular to its plane. In the rotating frame, the excitation appears as the rotating force

$$F_d = \delta(r - r_0)\delta(\theta + \Omega t)/r_0 \quad \ldots(30)$$

The modal force associated with the n- nodal diameter mode

$w_n(r,\theta) = R_n(r)\cos n\theta \quad \ldots(31)$ is

$$f_n = \iint F_d(r,\theta,t) w_n(r,\theta) dA = R_n(r_0)\cos n\Omega t \quad \ldots(32)$$

Resonant response (i.e. a critical speed) occurs when $n\Omega=\omega_n$ as noted previously. One would expect modes having any number of nodal diameters other than zero to become critical at some speed, but Renshaw and Mote [10] proved that one-nodal diameter modes of a rigidly supported disk never become critical. These modes, however, do become critical for the coupled disk – spindle system as discussed below.

We use the stationary force interpretation to characterize the disk critical speeds of the coupled system. The extended excitation vector $(\overline{f})$ associated with a stationary point force on the disk is

$$\overline{f} = [F_d\,000000]^T \quad \ldots(33)$$

The modal force associated with the uncoupled extended eigenfunctions $\overline{h_n}$ of Eq. (29) with $a_1$=1 and $a_2$=0 is

$$f_n = R_n(r_0)\cos n\Omega t \qquad n \neq 1 \quad \ldots(34)$$

which is identical to Eq.(32). Resonant response occurs when $n\Omega = \omega_n \;\; (n \neq 1)$, as for the rigidly supported disk. Because the uncoupled vibration modes $n \neq 1$ and corresponding rotating frame natural frequencies $\omega_n$ of a disk – spindle system are exactly those of rigidly supported disk [1[, the disk critical speeds of the uncoupled modes are unaffected by disk – spindle coupling. Thus the coupled system is subjected to the same critical speed instabilities as the rigidly supported disk; the unstable critical modes are identical to those of a rigidly supported disk and involve purely disk deformation.

Considering now the coupled vibration mode, $\overline{h_m}$ of Eq. (28), the associated modal force is

$$f_m = g_m(r_0)\cos\Omega t - p_m(r_0)\sin\Omega t \quad m = 1,2,3,.... \quad \ldots(35)$$

## Results and Discussion

A model of non-dimensional parameters listed below has been taken as a study case:

$K = 0.000355 \quad d_1 = 0.03248 \quad \gamma = 0.5 \quad J_{11}^c = 0.029521$

$\rho = 0.022279 \quad \alpha = 2.05774 \quad \upsilon = 0.28 \quad J_{22}^c = 0.029521$

$J_{33}^c = 0.057743 \quad J_{11}^d = 0.016404 \quad J_{22}^d = 0.016404 \quad J_{33}^d = 0.032808$

The choice of the point of expansion for the power series, Eq.(25) varies in the literature, Wu and Flowers [4] used the regular singular point r=0, whereas Eversman and Dodson [7] and Chivens and Nelson [3] used the ordinary point r=1. In order to check whether expansion about one point leads to better convergence than the other, an approach identical to that above used to obtain the natural frequencies by expanding about r=0.

This method, however, gave the first two natural frequencies, at each speed as shown in table(1), irrespective of the number of terms retained in the power series, moreover, the convergence for r=0 is slower than for r=1. The choice r=1 is superior to r=0 for the parameter set considered here, and the expansion about r=1 is used in the subsequent results.

**Table(1) Comparison of convergence of natural frequencies for power series expansion about r=0 and r=1**

| | | r=0 | | | | r=1 | | |
|---|---|---|---|---|---|---|---|---|
| | | Number Of Terms | | | | Number Of Terms | | |
| Ω | Galerkin | 20 | 40 | 60 | 80 | 20 | 40 | 60 |
| 0.5 | 0.593 | 0.593 | 0.593 | 0.593 | 0.593 | 0.593 | 0.593 | 0.593 |
| | 1.528 | 1.558 | 1.555 | 1.554 | 1.552 | 1.528 | 1.528 | 1.528 |
| | 1.844 | | | | | 1.884 | 1.844 | 1.844 |
| 1.0 | 0.113 | 0.114 | 0.113 | 0.113 | 0.113 | 0.113 | 0.113 | 0.113 |
| | 1.987 | 2.036 | 2.032 | 2.031 | 2.03 | 1.988 | 1.987 | 1.987 |
| | 2.267 | | | | | 2.268 | 2.267 | 2.267 |
| 2.0 | 0.852 | 0.87 | 0.852 | 0.852 | 0.852 | 0.852 | 0.852 | 0.852 |
| | 2.948 | 2.979 | 2.977 | 2.976 | 2.974 | 2.950 | 2.948 | 2.948 |
| | 3.457 | | | | | 3.458 | 3.457 | 3.457 |

The closed form solution (CFS) provides a valuable benchmark for evaluation of approximate methods. The comparison between the CFS and the Galerkin solution in Parker and Mote [6] is shown in Fig.(2). Only the natural frequencies of the coupled one-nodal diameter are shown . Excellent agreement with the CFS is observed for all eigenvalues even for extremely high speeds. The Galerkin solution employed 12 zero speed eigenfunctions (six degenerate pairs) as basis function at each speed. The CFS requires 40 terms to converge at Ω=2, as shown in table(1); more terms are necessary at higher speeds. Validation of the Galarkin results is important as Galerkin discretization is far more convenient than the CFS for the perspectives for programming size and computational efficiency. The accuracy of the Galarkin discretization can not be taken as granted in the absence of verifying CFS, however , as discretization methods for gyroscopic systems at high speeds may converge poorly and yield erroneous results [8,9]. An advantage of the Galerkin solution is that the inertia, gyroscopic and stiffness matrices are independent of speed and are calculated only once.

A key feature of the above complex, speed- dependent eigenfunctions is that they likely provide an excellent basis for discretization of models with non-linear, time-varying and dissipative effects that are present in practical systems. For example axially moving media system (which are gyroscopic system) demonstrate excellent convergence when complex, speed-dependent eigenfunctions are used in the discretization [8].

Resonance occurs for $\Omega=\omega_m$, this condition defines the disk critical speeds corresponding to the coupled modes. This condition is satisfied as is evident from Fig.(3), where the lowest critical speed is actually lower than the lowest spindle critical speed ($\Omega$=0). Thus in contrast to the rigidly supported disk, critical speed instabilities of the one-nodal diameter modes, which are the coupled modes of the disk – spindle system, do occur. The severity of a disk critical sped instability depend on whether the critical coupled mode involves predominately disk or spindle deformation. For the study case under hand the critical modes at all disk critical speeds are predominantly spindle modes. For these modes, the modal force given by Eq.(35) is small. As a result, the instability may be not severe in the light of small damping inherently present in the system that limits the resonant response amplitude. A more dangerous situation exists when the critical coupled mode is predominately a disk mode, as the resonant response induced by stationary disk forces would be driven by a larger modal force.

Figure(3) shows the variation the zero speed ($\Omega$=0) natural frequencies obtained by the CFS with the parameters ($k/k_0$), ($J_{ii}^{c,d}/J_{ii_0}^{c,d}$) and ($\alpha/\alpha_0$), where $K_0$, $J_{ii_0}^{c,d}$ and $\alpha_0$ are as in the parameters set listed in the study case.

In summary, spindle critical speeds exists at zero eigenvalues of the coupled system as viewed in the rotating frame. The critical modes are call coupled modes as pure spindle do not exist. Disk critical speeds exist for the uncoupled mode (pure disk deformation) at exactly the same critical speeds as for the rigidly supported disk, that is $\Omega_{cr}=\omega_n/n$. Disk critical speeds exist for the coupled modes when $\Omega=\omega_m$.

## Conclusions

1- A closed form analytical solution to the eigenvalue problem of the rotating disk – spindle system involving modal analysis is obtained. This solution provides a valuable benchmark for evaluation of approximate modes. Galerkin discretization provides excellent results for eigensolutions.

2- For the parameters set considered, the convergence of power series solution to the disk equation is markedly better for expansion about r=1 than about the regular singular point r=0. While the limited parameter range considered here does not permit general convergence conclusions, the large difference suggest superiority of the expansion about r=1.

3- Disk critical speeds analogous to those of rigidly supported rotating disk exist in addition to spindle critical speeds associated with vanishing eigenvalues. Futhermore, disk – spindle coupling introduces disk critical speeds associated with the one-nodal diameter coupled modes that do not exist for a rigidly supported disk. The critical speeds of rigidly supported disk corresponding to the modes with numbers of nodal diameters other than one remain points of instability; these speeds are unaffected by disk – spindle coupling.

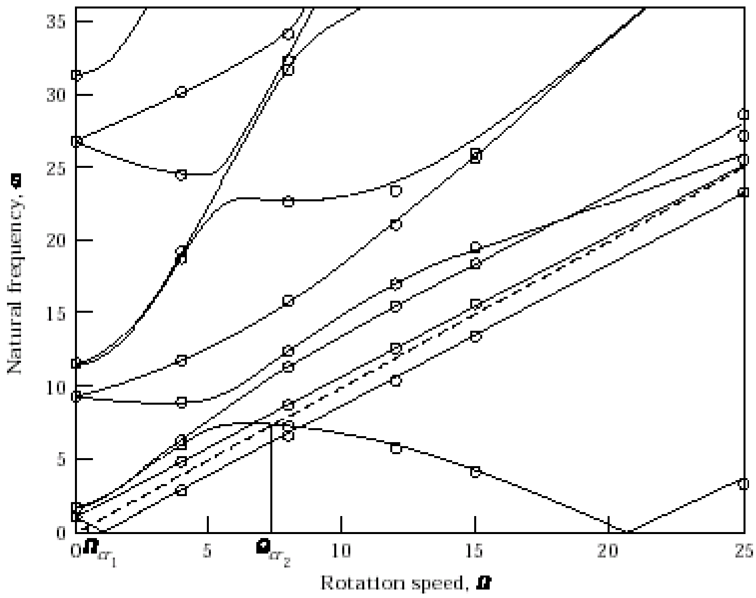


**Figure(2): Comparison between the CFS (denoted by circles) and Galerkin (denoted by solid curves) natural frequencies. The dashed line has unity slope, it's points of intersection with the solid lines are the disk critical speeds $\Omega_{cr}$**

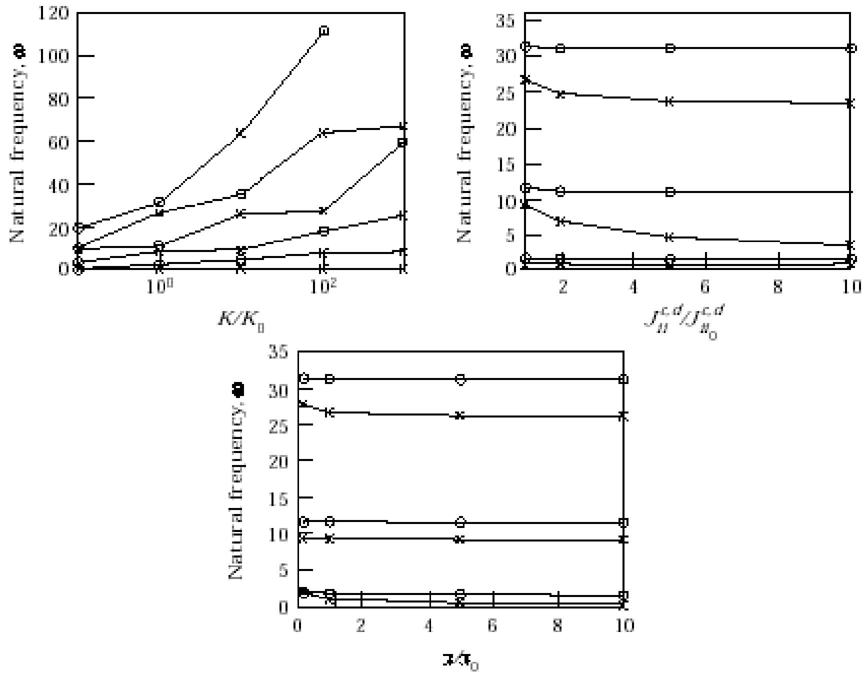


**Figure(3): Variation of the zero natural frequencies with some non-dimensional parameters. The circles denote spindle natural frequencies while the crosses denote disk natural frequencies.**

## Nomenclature

| | |
|---|---|
| a,b | Inner and outer radii of the disk respectively (m) |
| D | Disk flexural rigidity (N.m) |
| $\overline{d}$ | Clamp half thickness (m) |
| EI | Spindle bending stiffness (N.m$^2$) |
| $\overline{F_i}$ | Applied force on the clamp (N) |
| $\overline{J_{ii}^c}, \overline{J_{ii}^d}$ | Mass moment of inertia of the clamp and the disk respectively (Kg.m$^2$) |
| K | Extensional (stretching ) rigidity |
| l | Length of the spindle (m) |
| $m$ | Combined mass of the clamp and the disk (Kg ) |
| $\overline{M_i}$ | Applied moment on the clamp (N.m ) |
| $\overline{q_d}$ | Transverse force per unit area of the disk N/m$^2$ |
| $\overline{q_u}$ | Horizontal transverse force per unit length of the spindle (N/m) |
| $\overline{q_v}$ | Vertical transverse force per unit length of the spindle (N/m) |
| $\bar{t}$ | Time (sec) |
| $u(z,t)$ | Horizontal elastic deflection of the spindle (m) |
| $u^c(t)$ | Horizontal displacement of the clamp's center of mass (m) |
| $v(z,t)$ | Vertical elastic deflection of the spindle (m) |
| $v^c(t)$ | Vertical displacement of the clamp's center of mass (m) |
| $w(r,\theta,t)$ | Transverse elastic deflection of the disk (m) |
| $\varphi(t)$ | Clamp rotation in the plane of horizontal elastic deflection $u$ |
| $\psi(t)$ | Clamp rotation in the plane of vertical elastic deflection $v$ |
| $\overline{\Omega}$ | Rotation speed (rad/sec) |
| $\upsilon$ | Poisson's ratio |
| $\rho_d$ | Disk mass per unit area (Kg/m$^2$) |
| $\rho_s$ | Spindle mass per unit length (Kg/m) |
| $\sigma^{r,\theta}$ | Disk rotational stresses in the radial and circumferential directions respectively (Pas) |
| $\delta$ | Dirac delta function |
| $\omega_m$ | The natural frequency of the coupled modes (rad/sec) |
| $\omega_n$ | Rotating frame natural frequency of the uncoupled modes (rad/sec) |

## References


1- R.G. Parker "Analytical vibration of spinning elastic disk – spindle system" J. of applied mechanics, 1999,(66), p 218-224.

2- J.A. Dopkin and T.E. Shoup " Power resonant speed reduction caused by flexibility disks " J. of engineering for industry, 1974,(96), p 1328-1333.

3- D.R. Chivens and H.D. Nelson " The natural frequencies and critical speeds of a rotating flexible shaft – disk system " J. of engineering for industry, 1975, (97), p.881-886.

4- F.S. Wu. and G.T. Flowers “ A transfer matrix technique for evaluating the natural frequencies and critical speeds of a rotator with multiple flexible disk” J. of vibration and acoustics, 1992,(114), p 242-248.
5- S.P. Timoshinko and J.N.Goodier “ Theory of elasticity “ 1982, international student edition.
6- R.G. Parker and C.D. Mote “ Vibration and coupling phenomena in a symmetric disk – spindle system “ J. of applied mechanics, 1996, (63), p 953-961.
7- W. Eversman and R.O. Dodson “ Free vibration of a centrally clamped spinning circular disk “ J. of AIAA, 1969,(7),p 2010-2012.
8- J.A.Wickert and C.D. Mote “ Response of discretization methods for axially moving materials “ J. of applied mechanics review, 1991, (44), p s279- s284.
9- R.G. Parker “Supercritical speed stability of the trivial equilibrium of an axially moving string on an elastic foundation" J. of sound and vibration, 1999, 221(2), p 205-219.
10- A.A. Renshaw and C.D. Mote “ Absence of one nodal diameter critical speed modes in an axisymmetric rotating disk “ J. of applied mechanics, 1992, (59), p 687-691.
11- L. Meirovitch "A modal analysis for the response of linear gyroscopic system" J. of applied mechanics,1975,(42),p 446-450.
12- G.M.T. Deleuterio and P.C.Hughes "Dynamics of gyroscopic continua" J. of applied mechanics, 1984, (51), p 415 – 422.
13- C. Ray Wylie " Advanced engineering mathematics " international student edition, 1975.

# حل مغلق الشكل للخواص الاهتزازية الحرة لمنظومة قرص دوار مع عمود دوار قصير

**الخلاصة**

أن منظومة القرص الدوار مع عمود دوار قصير تتكون من قرص مرن مركب على عمود دوار قصير مرن بواسطة مثبت صلب. أن هذا العمل يقدم حل مغلق الشكل للحلول الأيكنية(*) لهكذا أنظمة. أن الدوال الأيكنية المعقدة تمتلك الخواص الكلاسيكية لمنظومة الجايروسكوب عندما تجمع الانحرافات المنفردة للقرص, العمود الدوار القصير و المثبت لدالة أيكنية معينة بدلالة الدوال الأيكنية الممتدة.

أن السرع الحرجة المشابهة إلى تلك الموجودة في القرص الدوار ذو الإسناد الصلب (الكلاسيكي) قد اختبرت لمنظومة مزدوجة.

لقد تم التوصل إلى أنه بينما القرص الدوار ذو الإسناد الصلب لا يكشف عن عدم أستقرارية عند السرعة الحرجة في الدالة الأيكنية ذات العقدة الواحدة القطرية, فأن المنظومة المزدوجة قد أظهرت ذلك.

(*) لم نعرف الترجمة العربية لكلمة eigen حيث لم نجد لها أية ترجمة في القواميس المتوفرة.